ARTICLE

OBC
www.rsc.org/obc

# Kinetic and thermodynamic consequences of the substitution of SMe for OMe substituents of cryptophane hosts on the binding of neutral and cationic guests† ‡

**Chantal Garcia, Delphine Humilière, Nathalie Riva, André Collet and Jean-Pierre Dutasta ***
*Stéréochimie et Interactions Moléculaires, École Normale Supérieure de Lyon, UMR CNRS N°5532, 46 Allée d'Italie, F-69364 Lyon 07, France. E-mail: dutasta@ens-lyon.fr*

***Received 19th November 2002, Accepted 1st May 2003***
***First published as an Advance Article on the web 12th May 2003***

To investigate the origin of the high selectivity of cryptophane-E (**1**) towards $Me_3NH^+$, $Me_4N^+$, and $CHCl_3$, and particularly to discriminate the different contributions that stabilize the supramolecular complexes, we have synthesized the new cryptophane **2** bearing six MeS groups instead of MeO groups in **1**. This led to a decrease of the negative charge density in the equatorial region of **2** without affecting notably the size of the molecular cavity. The binding properties of **1** and **2** towards the three guests were examined in solution and showed a slight decrease of the $\Delta G_a$ favoring the complexes of **1**, accompanied by a significant modification of the $\Delta H_a$ *vs.* $\Delta S_a$ balance. The binding of the ammonium guests to **1** and **2** was strongly entropy driven, while that of $CHCl_3$ was purely enthalpy driven. A combination of spectroscopic and computational techniques was used to assign the main intermolecular interactions that occurred during the inclusion process. The neutral $CHCl_3$ molecule is more stabilized in the less negatively charged CTV cap of **1**. The different behavior towards the ammonium cations can be explained in term of interactions with the electronegative heteroatoms and cation–π interactions. Moreover, this study revealed a considerable slowing down of the guest exchange kinetics with host **2**, for which the association and dissociation rates are reduced by a factor $10^3$ to $10^4$ with respect to **1**. For example, at room temperature, the $Me_4N^+$@**2** complex exhibits a half-life of *ca.* 2 years, instead of a few hours for the corresponding complex of **1**.

## Introduction

The host–guest concept is by far the best approach to generate new molecular devices and so far recognition of guests by artificial hosts has received much interest. The reversible encapsulation of various substrates in molecular capsules, cavitands or carcerands has allowed the formation of novel supramolecular assemblies, used in the design of new materials.[1–16] Associated with this synthetic work, progress has been undertaken to understand the recognition phenomena and to measure the kinetic and thermodynamic parameters of the supramolecular associations. The cryptophanes[17,18] (see Chart 1) represent a family of cyclophane hosts[19] known for their ability to form stable inclusion complexes with a variety of neutral and cationic molecules.[20–28] These studies have recently been extended to monoatomic xenon, which proved to bind to the smallest cryptophanes with an exceptionally large affinity in organic solvents.[29–32] These artificial host–guest (H–G) systems represent useful tools to study the mechanisms of molecular recognition, because they display association or dissociation equilibria (H + G ⇌ HG) that are easily observable and well characterized by NMR techniques. In addition, representative X-ray structures of the complexes have been solved, and sophisticated simulations have been performed to reveal some of the dynamic aspects of the molecular recognition that are not easy to observe experimentally.[33–36] The present work was undertaken to gain some insight into the factors responsible for the selectivity of cryptophane-E (**1**) towards $Me_3NH^+$, $Me_4N^+$, and $CHCl_3$, for which values of association constants $K_a$ = 1500, 225 000, and 470 $M^{-1}$ [$(CDCl_2)_2$, 300 K] had been measured.[37] At the time these studies were first reported, the amazing stability of the $Me_4N^+$ complex ($\Delta G_a$ −30.9 kJ $mol^{-1}$) was ascribed to cation–π interactions,[38] the magnitude of which had been evaluated by Schneider and coworkers at 4.2–5.4 kJ $mol^{-1}$ per interacting aromatic ring.[39] This figure has recently been challenged by Roelens and Torriti who have proposed a value of 2 kJ $mol^{-1}$ per aromatic ring, with a saturation limit around 8 kJ $mol^{-1}$.[40] If these views are correct, then the earlier explanation of the affinity of **1** towards $Me_4N^+$ should be revised.

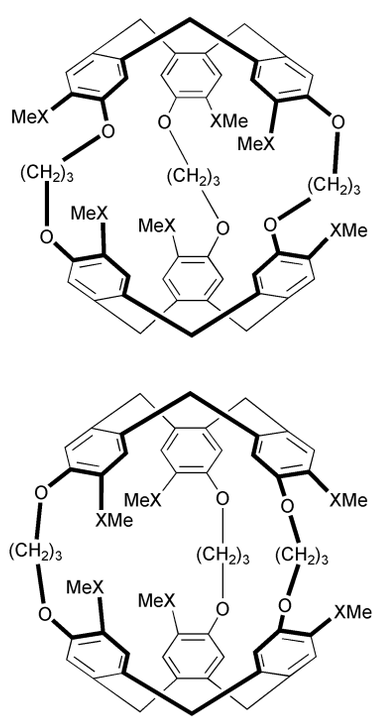


**Chart 1**

In order to shed light on the nature of the interactions between the cryptophane and its guests, we have made a small

† Dedicated to the memory of Professor André Collet deceased on October 1999.
‡ Electronic supplementary information (ESI) available: kinetics of complexation. See http://www.rsc.org/suppdata/ob/b2/b211363e/

DOI: 10.1039/b211363e

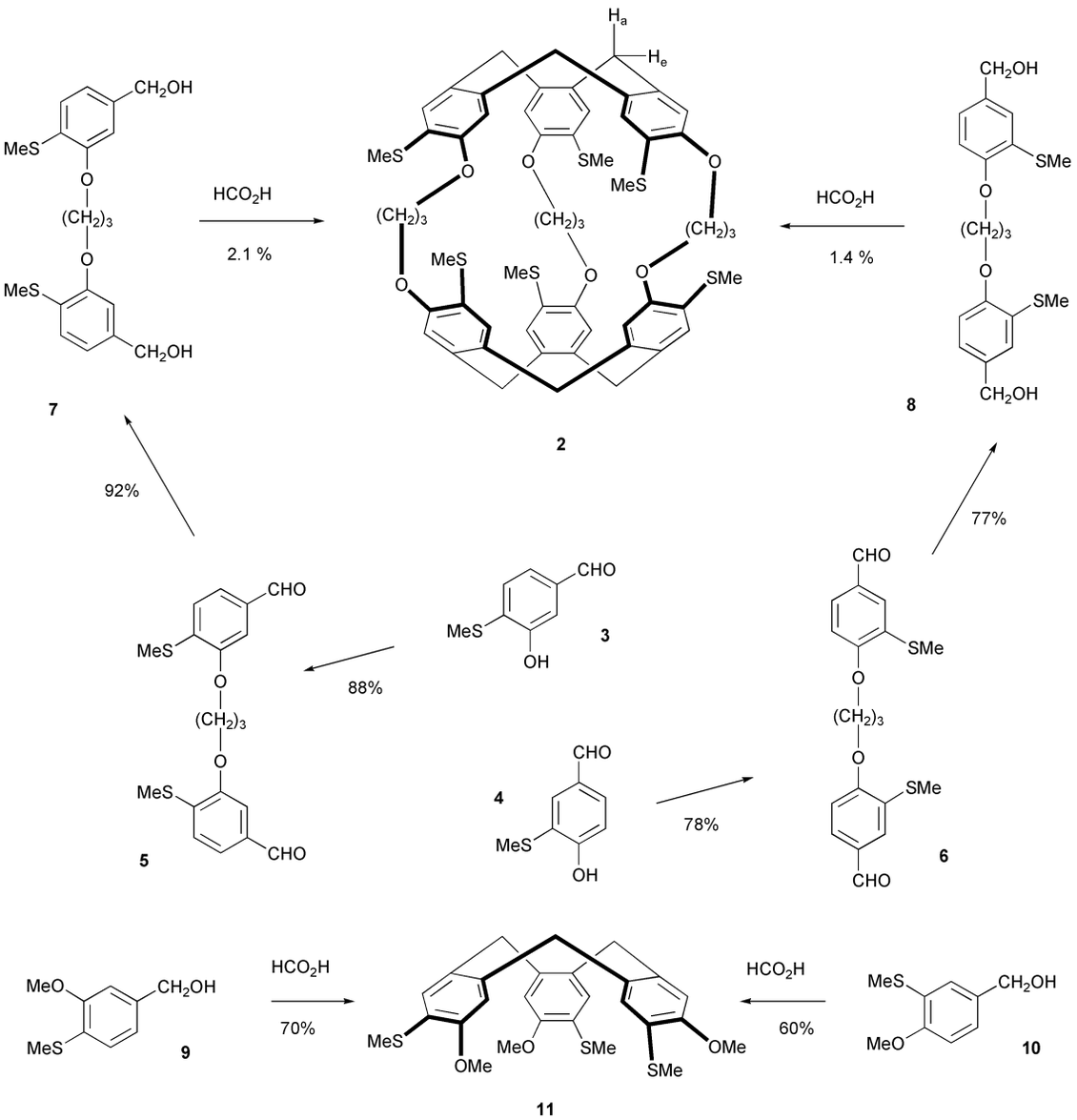


**Chart 2**

structural modification of **1**, and we have examined the effect this perturbation has on the various thermodynamic and kinetic parameters, which describe the behavior of the system. This approach has the advantage that solvent contributions can be minimized as solvation effects are very close for the parent cryptophane and the modified form. In this paper, we describe the synthesis and structural characterization of the new cryptophane **2**, in which six less electronegative SMe groups have replaced the six OMe substituents of **1**. Although the bulkier SMe groups encumber the windows of the cryptophane host, on going from OMe to SMe substituents does not modify the size of the inner cavity of the cryptophane. This modification is in fact designed to probe the effect of a decrease of the negative charge density in the equatorial region of the cryptophane on the properties of its inclusion complexes. This synthetic work is followed by a detailed investigation of the interaction of **1** and **2** with $Me_3NH^+$, $Me_4N^+$ and $CHCl_3$, a neutral guest isosteric with $Me_3NH^+$, which shows a reversed surface polarity.

## Results

### Synthesis of cryptophane 2

The cryptophane bearing MeS peripheral substituents was prepared by the sequence shown in Chart 2, which is similar to that used for the preparation of the parent compound **1**.[41] This method normally produces the *anti* $D_3$ isomer (*e.g.*, **1**), with an excellent selectivity with respect to the corresponding *syn* $C_{3h}$ isomer (**1′**; see Chart 1). The key step in this synthesis is the double trimerization of a bis-benzylalcohol such as **8**, in which the $CH_2OH$ groups precursor of the benzyl cations involved in the reaction are situated *para* to the $O(CH_2)_3O$ spacer. Reaction of isothiovanillin **4**[42] with 1,3-dibromopropane followed by reduction of the intermediate dialdehyde **6** furnished the desired diol **8** in 60% overall yield. The conversion of **8** to **2** was carried out by reaction in formic acid containing a small amount of $CHCl_3$ to ensure dissolution of the diol, and gave **2** in 1.4% yield. This yield is much lower than that obtained in the similar synthesis of **1** (*ca.* 15%).

In an attempt to improve on this, we examined the effect of moving the $CH_2OH$ groups of the precursor to a position *para* to the MeS groups. The diol **7** was thus prepared in 81% yield from thiovanillin **3**,[41] using the same sequence as for the preparation of **8**. Reaction of **7** with formic acid afforded cryptophane **2** in 2.1% yield. This detrimental influence of the MeS groups on the formation of the cryptophane was not expected. Earlier works have shown that MeS substituents do not prevent the conversion of benzyl alcohols to cyclotriveratrylenes. Thus, in the presence of formic acid, both the (3-MeO, 4-MeS) benzyl alcohol **9** and its (3-MeS, 4-MeO) regioisomer **10** have been

converted to the corresponding $C_3$-cyclotriveratrylene **11** in 70% and 60% yield, respectively.[42] The larger steric requirement of MeS *vs*. MeO is possibly responsible for the effect of making more difficult the formation of the postulated ribbon-like intermediate that eventually cyclizes to the cryptophane structure.[18]

The *anti* structure was evidenced by $^1$H-NMR, which displayed a broad singlet for the inner $CH_2$ protons of the $O(CH_2)_3O$ bridges (Fig. 1). In the $D_3$ *anti* isomer **2** this $CH_2$ lies on a $C_2$ axis and its two hydrogens are homotopic; the observed broadening is due to the coupling with the adjacent $CH_2$ groups and probably to the conformational mobility of the spacer bridges. In the $C_{3h}$ *syn* isomer these hydrogens are diastereotopic and would give two separate signals, as observed in cryptophane-F **1′**. A further confirmation of this assignment was provided by HPLC analysis of the cryptophane using a chiral stationary phase (Chiralpak-OT$^+$), which showed a resolution into two peaks of equal intensity, corresponding to the enantiomers of **2** (the *syn* isomer is achiral).[43]

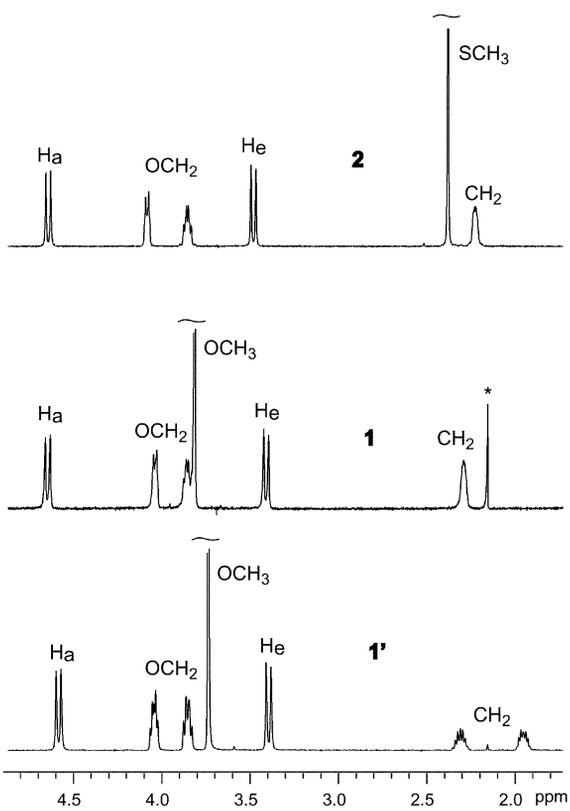


**Fig. 1** Part of the 500 MHz $^1$H-NMR spectra of **1**, **2** and **1′** in $CDCl_3$, showing the differences between *anti* and *syn* isomers.

### Preliminary complexation studies

Crystalline complexes of **1** and **2** with $CHCl_3$ were obtained by evaporating to dryness solutions of the hosts in this solvent. The G : H ratio of these solid samples was close to 2 : 1, one of the $CHCl_3$ molecules being incarcerated within the host cavity, the other being located in voids of the crystal lattice.[44] When such complexes were dissolved in $(CDCl_2)_2$, the $^1$H-NMR spectra recorded at room temperature exhibited two separate signals for the free ($\delta$ 7.29 ppm) and bound $CHCl_3$ ($\delta$ 2.86 for **1**, 2.90 for **2**). With host **1**, the free–bound guest ratio did not change with time and showed an immediate response to temperature changes. This means that the guest exchange between the solvent and the host cavity, which is slow on the spectrometer time scale,[45] is nevertheless sufficiently fast to allow the equilibrium to be reached during the experiment time. In this case, the association constant $K_a$ and its variations with temperature can be measured in a direct way, and the exchange rate can be deduced from lineshape analysis of the free and bound guest signals,[46] or NOESY experiments. When the same experiments were attempted on the $CHCl_3$@**2** system, the first spectrum we could record *ca.* 7 min after dissolution of the crystalline complex in $(CDCl_2)_2$ at 20 °C, showed 85% of the host molecules containing a $CHCl_3$ guest in their cavity (Fig. 2). The amount of complex then slowly decreased, to reach a constant value of 38% after *ca.* 100 min.

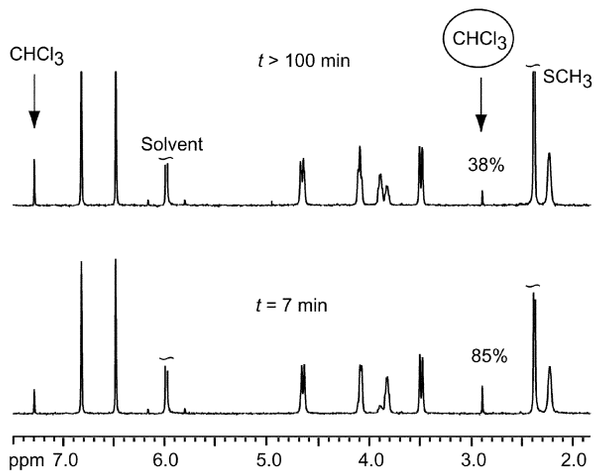


**Fig. 2** 500 MHz $^1$H-NMR spectra of **2** in $(CDCl_2)_2$, 20 °C; the slow dissociation of the $CHCl_3$ complex is evidenced by the spectra recorded 7 min (85% of complex) and 100 min (38%) after dissolution of a crystalline complex of composition [**2**, 1.6 $CHCl_3$].

Upon addition of $Me_3NH^+$ picrate to a solution of empty **1** at 298 K, the complex forms immediately, and is evidenced by the presence of a doublet at −0.36 ppm and a broad signal at 0.73 ppm representing the $N(CH_3)_3$ and NH resonances of the incarcerated guest, respectively. The corresponding resonances of the free guest are observed as two singlets at 2.94 ppm and 11.2 ppm. The coupling between the $N(CH_3)_3$ and NH hydrogens ($^3J$ = 5 Hz), which is observable in the complex, is not seen in the free guest due to a too fast intermolecular exchange of the NH proton. Most of the cryptophane resonances are shifted downfield upon complexation, and the free and complexed hosts are clearly visible in the spectrum. The largest shift (+0.08 ppm) is observed for the inner $CH_2$ of the spacer bridges; the OMe groups, the aromatic hydrogens, and the $H_e$ of the methylene bridges are also significantly shifted. The $Me_3NH^+$ complex of **2** formed at a much lower rate. The $^1$H-NMR chemical shifts of the $Me_3NH^+$@**2** complex indicate that its structure must be very similar to that of **1**. The incarcerated $Me_3NH^+$ shows a doublet ($^3J$ = 5 Hz) at −0.33 ppm ($Me_3N$) and a broad signal at 0.83 ppm (NH), and most of the cryptophane resonances are downfield shifted. The largest shift (*ca.* +0.1 ppm) is observed for the inner $CH_2$ of the spacer bridges. The binding of $Me_4N^+$ picrate to host **1** was still relatively fast at room temperature. The free and bound guest signals appear as sharp singlets at 3.35 and −0.26 ppm, respectively. After *ca*. 30–40 min, the signal of the free guest was no longer detectable and only the peak corresponding to the complexed guest remained. This means that the association constant was too large to be measured in this experiment. Thus, competition experiments with $Me_3NH^+$ and $Me_4N^+$ as guests, were performed. The association of $Me_4N^+$ to host **2** was considerably slower than its binding to host **1**. At the beginning of the experiment, the signals of the free guest (3.37 ppm) and of the bound guest (−0.24 ppm) were both present. After *ca*. 55 h, only the signal of the bound guest was visible, which means that in this case also the value of $K_a$ is too large to be measured directly, and was determined from competition experiments.

It is thus obvious that the guest exchange rate is considerably slower with **2** than it is with **1**, a situation that has never been

**Table 1** Kinetic parameters for association and dissociation of $CHCl_3$ and ammonium picrates in the presence of hosts **1** and **2** at 293 K in $(CDCl_2)_2$

| Guest | Host | $k_a$/$M^{-1}$ $s^{-1}$ | $k_d$/$s^{-1}$ | $\Delta G_a^{\ddagger}$/kJ $mol^{-1}$ | $\Delta G_d^{\ddagger}$/kJ $mol^{-1}$ | $(t_{1/2})_\infty$ [a] |
|---|---|---|---|---|---|---|
| $CHCl_3$ | **1** | 760 | 1.27 ([b]) | 55.6 | 71.2 | 0.55 s |
| | **2** | $1.16 \times 10^{-1}$ | $4.88 \times 10^{-4}$ | 77.0 | 90.4 | 24 min |
| $Me_3NH^+$ | **1** | 76.6 | $4.81 \times 10^{-2}$ | 61.9 | 79.2 | 14 s |
| | **2** | $2.32 \times 10^{-3}$ | $1.99 \times 10^{-6}$ | 86.6 | 103.8 | 97 h |
| $Me_4N^+$ | **1** | 7.2 | $1.49 \times 10^{-5}$ | 67.8 | 98.7 | 13 h |
| | **2** | $2.88 \times 10^{-3}$ | $1.0 \times 10^{-8}$ | 85.4 | 116.3 | 792 days |

[a] Half-life of the complex at infinite dilution. [b] Measured from lineshape simulation of the free and complexed guest signals.[37]

encountered in cryptophane complexes so far. In the following experiments, the rate of dissociation can be measured by recording NMR spectra as a function of time, using the kinetic model defined below. The rate of association can similarly be measured either by adding an excess of guest to a system already in equilibrium, or by adding the guest to a solution of *empty* host in $(CDCl_2)_2$.

### Kinetic model

We assume that the behaviour of these cryptophane–guest systems can be analysed in terms of H + G $\rightleftharpoons$ HG equilibria, where the forward reaction (association) is second order (rate constant $k_a$ in $M^{-1}$ $s^{-1}$) and the reverse reaction (dissociation) is first order ($k_d$ in $s^{-1}$). The $k_a/k_d$ ratio represents the equilibrium (association) constant $K_a$ (in $M^{-1}$). Accordingly, the rate of formation or of dissociation of the complex is expressed by eqn. (1).

$$\frac{d[\mathrm{HG}]}{dt} = k_a[\mathrm{H}][\mathrm{G}] - k_d[\mathrm{HG}] \qquad (1)$$

Integration of this differential equation in the general case led to kinetic equations for both association and dissociation processes (see Supplementary Information). ‡ A way to quantify the kinetic stability of the complex is to determine its half-life time $(t_{1/2})_\infty = \ln 2/k_d$, which only depends on $k_d$, and would be observed for a 1st order decay at infinite dilution, where the reverse reaction is negligible. Relevant kinetic parameters for all investigated complexes are assembled in Table 1.

### Kinetic data for $CHCl_3$, $Me_3NH^+$ and $Me_4N^+$ interacting with hosts 1 and 2

Measurements performed in the present work on the $CHCl_3$@**1** system yielded thermodynamic and kinetic values in good agreement with the earlier ones derived from line-shape simulation of the $^1$H-NMR guest signals.[23] At 293 K, the equilibrium is reached within a few seconds. As said above, this is no longer the case for the $CHCl_3$ complex of **2**. Fig. 3 shows the rates of association and dissociation for this system at 293 K, derived from $^1$H-NMR experiments. In both cases the equilibrium was attained after *ca.* 100 min, allowing the determination of the association constant $K_a = 240$ $M^{-1}$ or 241 $M^{-1}$ (±10%), from the dissociation or association experiments, respectively ($K_a$ = 600 $M^{-1}$ for the same complex of **1**). The fit of the experimental data to kinetic equations yielded the rate constants $k_a = 0.116$ $M^{-1}$ $s^{-1}$ and $k_d = 4.88 \times 10^{-4}$ $s^{-1}$, respectively. The lifetime $(t_{1/2})_\infty$ of the $CHCl_3$ complex of **2** at 293 K is thus of the order of 24 min, instead of 0.55 s for the same complex of **1**. In terms of $\Delta G^{\#}$, the barriers for association and for dissociation of the $CHCl_3$ complex are increased by approximately 20 kJ $mol^{-1}$ on going from **1** to **2**.

At 298 K, the equilibrium association constant for the $Me_3NH^+$@**1** complex was $K_a$ = 1535 $M^{-1}$ ($\Delta G_a = -18.2$ kJ $mol^{-1}$). At 275 K, the rate of association became slow enough to be measured (Fig. 4(a)). The equilibrium is attained after approximately 30 min, allowing to calculate the association

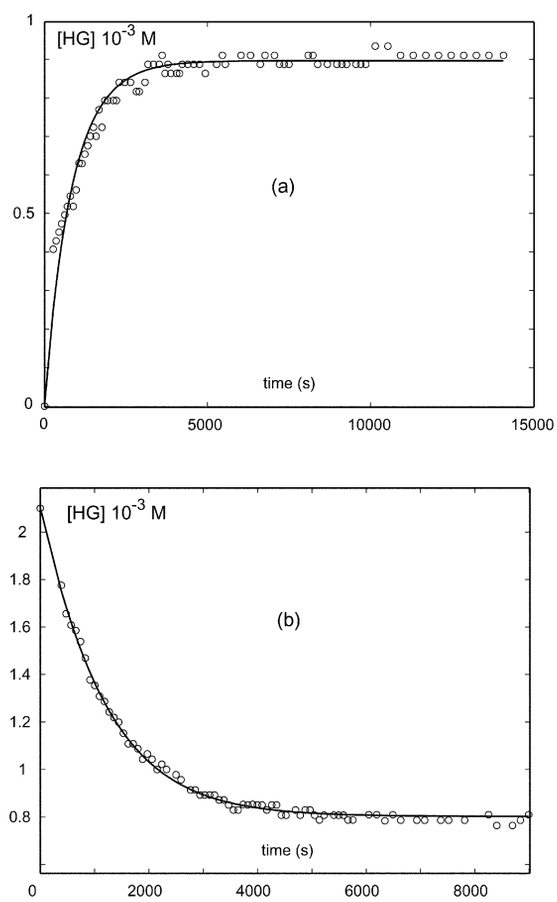


**Fig. 3** Association (a) and dissociation (b) kinetics for the $CHCl_3$ complex of **2** in $(CDCl_2)_2$, 293 K. In (a) the host concentration was 2.18 × $10^{-3}$ M and 1.8 eq. of $CHCl_3$ was added; in (b), the initial complex concentration was 2.1 × $10^{-3}$ M, and 0.6 eq. of free $CHCl_3$ was present.

constant, $K_a = 1700$ $M^{-1}$, and the rate constants, $k_a = 9.16$ $M^{-1}$ $s^{-1}$ and $k_d = 5.39 \times 10^{-3}$ $s^{-1}$. From these data the association and dissociation barrier were calculated to be $\Delta G_a^{\#} = 61.9$ and $\Delta G_d^{\#}$ = 79.2 kJ $mol^{-1}$, respectively. The $(t_{1/2})_\infty$ at 275 K is thus 130 s. Assuming that the barriers do not depend much on temperature, the rate constants and $(t_{1/2})_\infty$ at 293 K can be estimated from the Eyring equations, yielding a lifetime of 14 s for this complex at room temperature (Table 1).

The corresponding $Me_3NH^+$ complex of cryptophane **2** formed at a much slower rate (Fig. 4(b)). At 313 K, the equilibrium is reached after *ca.* 15 h (60.6% of complex, $K_a$ = 740 $M^{-1}$). The data shown in Fig. 4(b) were fitted to give the rate constants $k_a = 2.39 \times 10^{-2}$ $M^{-1}$ $s^{-1}$ and $k_d = 3.25 \times 10^{-5}$ $s^{-1}$ (313 K). The dissociation barrier is thus $\Delta G_d^{\#} = 103.8$ kJ $mol^{-1}$, *i.e.*, 24 kJ $mol^{-1}$ higher than for the complex of **1**. The estimated $(t_{1/2})_\infty$ at 293 K is 97 h (Table 1).

At 280 K, the rate of association of $Me_4N^+$ picrate salt to host **1** was slow enough to be measured by recording the intensities of suitable NMR peaks as a function of time (Fig. 5(a)). Since the association constant of $Me_3NH^+$ to **1** and

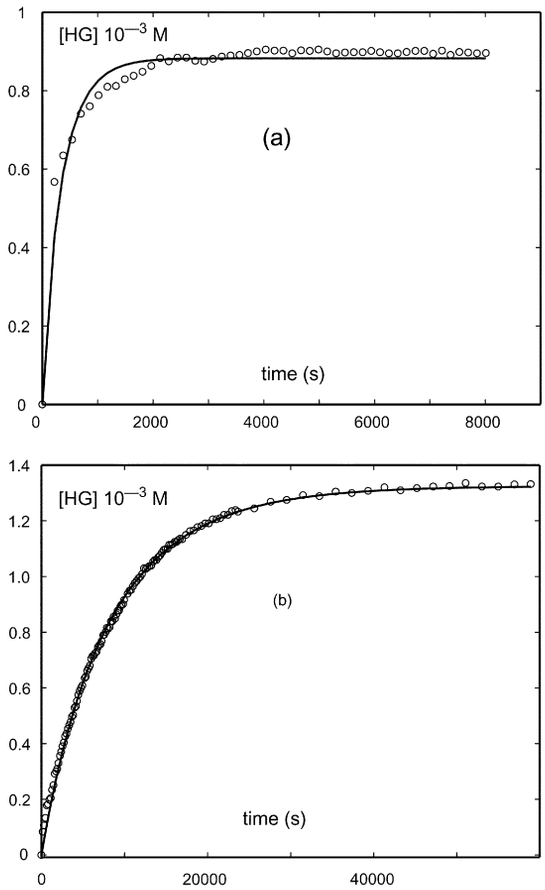


**Fig. 4** Kinetic of host–guest association upon addition of $Me_3NH^+$ ($picrate^-$) to a solution of empty cryptophane **1** or **2** in $(CDCl_2)_2$, and fit of the experimental points to eqn. (2); (a) host **1** ($2.61 \times 10^{-3}$ M), 0.45 eq. of guest added, 275 K; (b) host **2** ($2.19 \times 10^{-3}$ M), 1.5 eq. of guest added, 313 K.

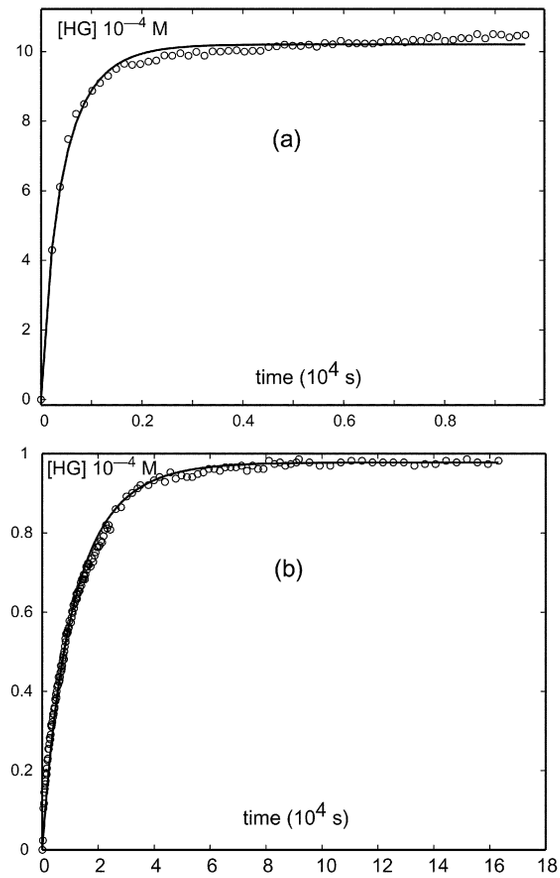


**Fig. 5** Kinetics of host–guest association upon addition of $Me_4N^+$ ($picrate^-$) to a solution of empty cryptophane **1** or **2** in $(CDCl_2)_2$, and fit of the experimental points to eqn. (2); (a) host **1** ($2.17 \times 10^{-3}$ M), 0.45 eq. of guest added, 280 K; (b) host **2** ($2.83 \times 10^{-3}$ M), 0.35 eq. of guest added, 313 K.

its variation with temperature can be easily measured, competition experiments with $Me_3NH^+$ and $Me_4N^+$ as guests, were performed in the range 293–323 K. The $K_a$ value at 300 K was thus found to be around 430 000 $M^{-1}$, a figure twice as large as that previously reported.[27] The new value is more reliable than the earlier one, because the conditions used in the present work allow a better precision in this determination. Using the same kinetic treatment as above for the data of Fig. 5(a), the value of $\Delta G_d^{\#}$ for the dissociation of the $Me_4N^+$ complex of **1** is found to be 98.7 kJ $mol^{-1}$ and its lifetime $(t_{1/2})_\infty$ at 293 K is estimated at 13 h (Table 1).

Competition experiments were then performed between $Me_3NH^+$@**2** and $Me_4N^+$@**2** complexes to determine the value of $K_a$ for the $Me_4N^+$@**2** complex, which was found to decrease from *ca.* 283 000 $M^{-1}$ at 293 K to *ca.* 136 000 $M^{-1}$ at 313 K. The association of $Me_4N^+$ to host **2** at 313 K is shown in Fig. 5(b). Treatment of the data then furnished a dissociation barrier of 116.3 kJ $mol^{-1}$, which corresponds to a $(t_{1/2})_\infty$ slightly greater than *two years* at 293 K (Table 1). This system is particularly interesting due to its reversibility at elevated temperature, where the complex can easily be formed, and its quasi-irreversibility at room temperature. This circumstance may be exploited for investigating the dynamic of the guest inside the molecular cavity in the absence of guest exchange.

### Thermodynamic data for $CHCl_3$, $Me_3NH^+$ and $Me_4N^+$ interacting with hosts 1 and 2

For all systems the variation of $K_a$ was determined in a range of temperature sufficient to obtain significant $R\ln K_a$ *vs.* $(1/T)$ plots (Fig. 6). The values of $\Delta H_a$ and $\Delta S_a$, together with other relevant thermodynamic parameters are assembled in Table 2. All systems exhibit negative enthalpies of association (exothermic binding). A striking difference is observed for the corresponding entropies, which are negative with $CHCl_3$ and positive for the ammonium guests. This means that a discussion of the relative stabilities of the complexes in terms of their $\Delta G_a$ values at room temperature cannot provide information on the origin of the molecular recognition.

## Discussion

The slowing down of the exchange rates on going from **1** to **2** has almost no impact on the equilibrium H–G affinities. This conclusion can be drawn by observing that the association ($\Delta G_a^{\#}$) and dissociation ($\Delta G_d^{\#}$) barriers for each guest (Table 1) are in all cases increased by almost the same value on going from **1** to **2** (*ca.* 20, 25, and 18 kJ $mol^{-1}$ for $CHCl_3$, $Me_3NH^+$ and $Me_4N^+$, respectively). The rationale for this effect is probably the fact that the replacement of OMe by SMe substituents restricts the cross section of the host windows, without appreciable consequences on the cavity dimensions. This was verified by building a model of **2** from the X-ray structure of **1**,[23] and by allowing the two cryptophane models to relax to their nearest energy minimum (Tripos force field[47]) in the presence of the same incarcerated ammonium guest. The only significant structural differences between **1** and **2** are the longer C–S bonds in the latter (1.79 Å instead of 1.37 Å for C–O) and the fact that Ar–SMe rotates more freely than does Ar–OMe. The bulkier size of the SMe groups makes the cryptophane windows more narrow, increasing *in a similar way* the association and dissociation barriers. This means that the thermodynamic parameters assembled in Table 2 are meaningful to discuss the origin of the host–guest affinities in these systems. The absolute values

**Table 2** Thermodynamic parameters for complexation of $CHCl_3$ and ammonium picrates by hosts **1** and **2** at 293 K in $(CDCl_2)_2$[a]

| Guest | Host | $K_a/M^{-1}$ | $\Delta G_a$/kJ mol$^{-1}$ | $\Delta H_a$/kJ mol$^{-1}$ | $\Delta S_a$/J mol$^{-1}$ K$^{-1}$ |
|---|---|---|---|---|---|
| $CHCl_3$ | **1** | 600 | −15.6 | −27.0 | −39 |
| | **2** | 270 | −13.7 | −15.1 | −5 |
| $Me_3NH^+$ | **1** | 1600 | −18.0 | −2.4 | +53 |
| | **2** | 1120 | −17.1 | −12.2 | +17 |
| $Me_4N^+$ | **1** | 475000 | −31.8 | −10.7 | +72 |
| | **2** | 283000 | −30.5 | −20.2 | +35 |

[a] Errors on $K_a$ estimated as ±10%.

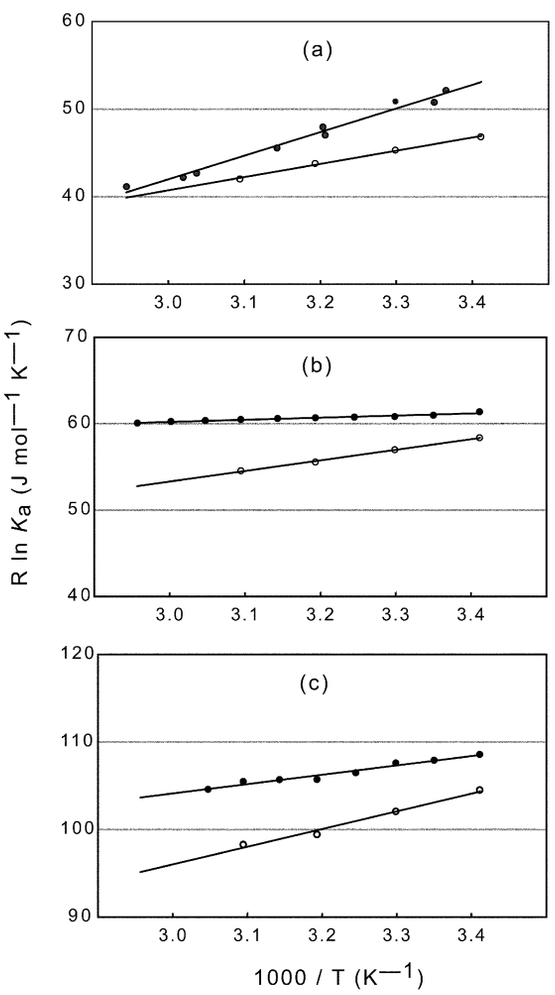


**Fig. 6** Van t'Hoff plots, with black circles for host **1**, open circle for host **2**; (a) $CHCl_3$; (b) $Me_3NH^+$ picrate; (c) $Me_4N^+$ picrate.

of these parameters comprise the enthalpy and entropy contributions for the transfer of the guest from the solvent to the host cavity. The magnitude of these solvophobic (or solvophilic) contributions is difficult to appreciate, particularly for the charged guests. By contrast, the changes of these parameters on going from **1** to **2** are totally free from the guest–solvent interactions. Under this condition it becomes possible to discuss the origin of the host–guest interactions by examining the effects that the structural changes of the host (*i.e.*, the replacement of OMe by SMe groups) have on the variation of the thermodynamic parameters of the complexes.

In order to evaluate the consequences the substitution of the SMe for the OMe groups have on the charge distribution around the cavity, *ab initio* calculations were performed on the simplified cyclotriveratrylene systems shown in Chart 3. Realistic models for **1** and **2** were built from the X-ray crystal structure of **1**.[23] In model **1**, the ether oxygens are negatively charged (−0.43 to −0.47), whereas the six aromatic carbons bear an overall negative charge of −0.21. The two aromatic hydrogens

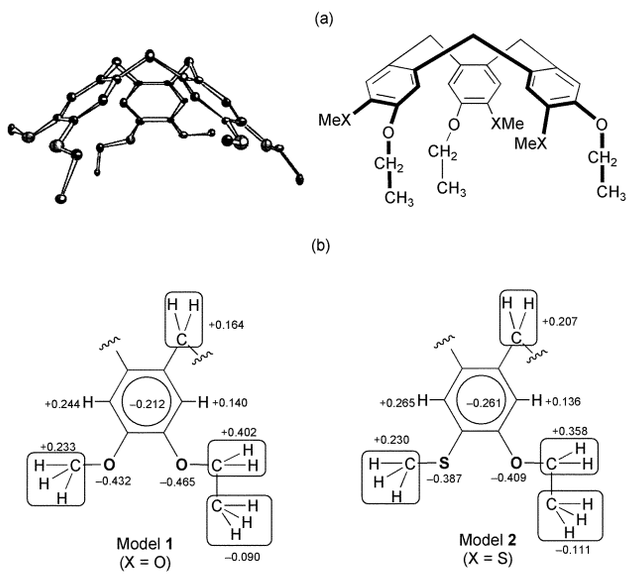


**Chart 3** (a) Models for cryptophanes **1** and **2** used for the charge calculations (X-ray conformation on the left); (b) CHELPG charges.

and the methylene bridges of the cyclotriveratrylene unit are distinctly positive. In model **2**, the heteroatoms are less negatively charged than in model **1**, −0.38 and −0.41 on the sulfur and oxygen atoms, respectively. In contrast, the aromatic carbons in model **2** are more negative than in model **1**: −0.26 *vs.* −0.21. These calculations suggest that the response of the H–G complex to the structural change must depend on the type of interactions the guest can develop with the host.

### The $CHCl_3$ complexes

We know from the crystal structure of the $CHCl_3$@**1** complex that the guest tends to align its $C_3$ axis with the North–South axis of the host. This exposes the guest hydrogen to the shielding effect of the three aromatic rings of one of the CTV caps, and explains the large upfield shift of 4.43 ppm observed for this hydrogen in the complex. The three chlorine atoms lie in the equatorial region, and make very short contacts to the aromatic carbons of the same CTV cap in which the C–H bond of the guest is embedded. The closest Cl–C contacts (3.3–3.5 Å) involve the aromatic carbons bearing the ether oxygens (the sum of the Van der Waals radii for C–Cl is 3.45 Å). Fig. 7 is a view of the X-ray structure of the complex, showing the way in which the guest is stuck to one of the host CTV caps, and evidencing the closest contacts. Thus, the less negatively charged CTV cap in **1** favors the $CHCl_3$@**1** complex as compared to the $CHCl_3$@**2** complex (Table 2). Consequently, we observed a reduced entropy loss in the $CHCl_3$@**2** that could be associated to a less organized assembly with **2** than with **1**.

### The $Me_3NH^+$ and $Me_4N^+$ complexes

Due to the lack of X-ray data for the ammonium complexes, we performed molecular mechanic calculations to get structural information on the ammonium@cryptophane assemblies.

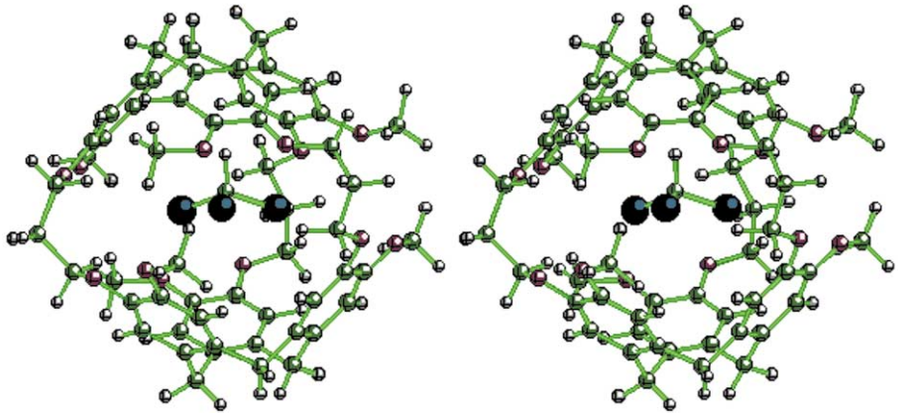

**Fig. 7** Stereoview of the X-ray structure of the $CHCl_3$@cryptophane **1** complex (ref. 23).

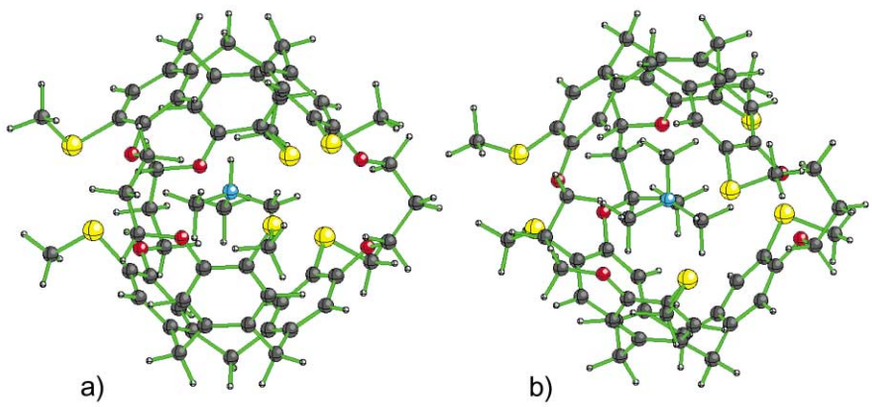


**Fig. 8** Molecular models of the (a) $Me_3NH^+$@**2** and (b) $Me_4N^+$@**2** complexes.

Starting with the known structure of the chloroform complex of **1**, energy minima were determined (Tripos force field[47]) for the $Me_3NH^+$@**1**, $Me_3NH^+$@**2**, $Me_4N^+$@**1** and $Me_4N^+$@**2** complexes. The minimized structures of the four complexes showed the guest located inside the molecular cavity with one N–H ($Me_3NH^+$) or one N–Me ($Me_4N^+$) bond aligned with the $C_3$ axis of the host (Fig. 8).

In the $Me_4N^+$ complexes the nitrogen atom is located in the centre of the cavity, whereas in the $Me_3NH^+$ complex it is shifted towards a CTV unit by about 0.3 Å. In the four complexes, the "axial" group aligned with the $C_3$ axis is in close contact with the aromatic rings of one CTV unit with distances of the $H_{ax}$ or $C_{ax}$ atom to the centroids of the benzene rings in the range 3.6–3.7 Å.

The distances to the heteroatoms are definitively larger. The $H_{ax}$ atom lies 4.4–4.7 Å from the oxygen atoms in both complexes and 4.95 Å from the sulfur atoms in $Me_3NH^+$@**2**. In the $Me_4N^+$ complexes the average distances of the $C_{ax}$ atom to the oxygen and sulfur atoms are 4.4 and 4.6 Å, respectively. For the three groups located in the "equatorial" region, the distances of the $C_{eq}$ carbons to the oxygen atoms are in the range 3.4–3.8 Å, and 3.6–4.2 Å for the distances to the sulfur atoms. The distances to the benzene rings are in the range 3.9–4.4 Å. Therefore, the major interactions of the three equatorial substituents mainly occur with the O or S atoms rather than with the aromatic cavity. The axial group contribution in the stability of the complex relies upon cation–π interactions, and can explain the stabilizing $\Delta H_a$ values observed with the ammonium complexes of cryptophane **2**, which contains a more negatively charged CTV unit, as compared to **1**. However, the remarkable stability of the ammonium-cryptophane complexes should result from both binding modes and a simple interpretation in terms of predominant cation–π interaction is not possible. With the ammonium@**2** complexes, the enthalpy–entropy compensation seems more relevant as the stabilizing of the complexes should increase the rigidity and organization of the assemblies. This is also in agreement with the larger size of the sulfur atoms, which congests the inner space of the host as compared to the oxygenated one. Moreover, the highest solvation of the charged guest compared to $CHCl_3$, and the need of the complete dissociation of the picrate salt for the encapsulation of the positively charged guest into the cavity of the cryptophanes, result in a more favorable entropy factor for the formation of the ammonium complexes.[48] This situation is totally different from the process described with open-shell cyclophane receptors, where the whole ion pair can be associated to the host, and consequently is essentially enthalpic in origin.[49]

## Conclusion

This work presents a detailed investigation about chloroform and ammonium recognition by cryptophanes. Introducing thiomethyl substituents on the cyclotriveratrylene units in the molecule, instead of the more common methoxy group, provided the new spherical host **2** with a comparable cavity to that of cryptophane-E **1**. The structural modifications came only from the larger MeS groups, which obstruct the portals of the host, and we have shown that this small modification in the host structure had significant changes in the complexation properties. This is evidenced by the higher values of the association and dissociation energy barriers (average $\Delta\Delta G^{\ddagger} = 21$ kJ mol$^{-1}$) measured for the different complexes of **1** and **2**. The half-life time $t_{1/2}$ are considerably increased for the guest@**2** complexes. For example, $t_{1/2}$ for $Me_4N^+$@**2** is $19 \times 10^3$ h instead of 13 h for $Me_4N^+$@**1** at 293 K in $(CDCl_2)_2$, acting so as a carcerand.[1] The binding of the ammonium guests to **1** and **2** was strongly entropy driven, while that of $CHCl_3$ was purely enthalpy driven. As the MeO (**1**) or MeS (**2**) cryptophanes are built upon the same aromatic architecture, the stability of the ammonium cations complexes were attributed to interactions with the

heteroatoms and cation–π effects, showing that the latter is not the unique stabilizing factor. These observations and their interpretations clearly illustrate the many challenges of host–guest chemistry, and justify the great interest of the cryptophanes as model systems allowing performing thorough experimental and theoretical studies for a better understanding of the molecular recognition processes.

## Experimental

Melting points were measured on a Perkin-Elmer DSC7 microcalorimeter. The $^1$H NMR spectra were recorded at 200 or 500 MHz on a Bruker AC200 and on Varian Unity$^+$ 500 spectrometers respectively. The $^{13}$C NMR spectra were recorded at 50 MHz on the Bruker AC200 spectrometer. Elemental analyses were performed by the Service Central d'Analyse du C.N.R.S. Column chromatographic separations were carried out over Merck silica gel 60 (0.040–0.063 mm); analytical and preparative thin-layer chromatography (TLC) were performed on Merck silica gel TLC plates F254.

### Complexation studies

The rate of association or dissociation of the various guests interacting with cryptophanes **1** and **2** as well as the corresponding equilibria were investigated by variable temperature $^1$H-NMR at 500 MHz in 1,1,2,2-tetrachloroethane-$d_2$. The peak of residual $C_2DHCl_4$ set to $\delta$ = 6.00 ppm was used as an internal standard. For $CHCl_3$ and $Me_3NH^+$ guests, the appropriate solutions were kept in the spectrometer throughout the experiment. In the case of $Me_4N^+$, the solution was kept in the spectrometer to record the beginning of the association or dissociation process, then it was transferred into a thermostated bath and the NMR spectra were recorded at regular intervals. Samples of empty hosts **1** or **2** can be prepared by evaporating to dryness, under vacuum, solutions of their $CHCl_3$ or $CH_2Cl_2$ complexes in $(CHCl_2)_2$. The $^1$H-NMR spectra of the empty cryptophanes **1** and **2** showed somewhat broadened signals, which were due to the existence of slowly exchanging conformations and to the presence in the host cavity of "invisible" guests such as atmospheric $N_2$ and (paramagnetic) $O_2$ molecules.

### Competition experiments

When the association constants were too large to be determined directly, competition experiments were performed. Host **1** ($2.18 \times 10^{-3}$ M) was allowed to interact with both $Me_3NH^+$ (1.25 eq.) and $Me_4N^+$ (1.05 eq.), and NMR spectra were recorded every 5 K in the range 293–323 K. After the equilibrium was reached (>1 day at 20 °C), the four peaks corresponding to the free and bound guests were visible, allowing to calculate the ratio of the binding constants and in turn the values of $K_a$ for $Me_4N^+$ in this temperature range. Similarly, NMR spectra of a solution of a mixture of host **2** ($2.83 \times 10^{-3}$ M), 1.03 eq. of $Me_4N^+$ and 3.46 eq. of $Me_3NH^+$, were recorded in the range 293–313 K. Several weeks were necessary to approach the equilibrium at 293K. The values of $K_a$ were then determined as for **1**.

### Kinetic model

Integration of the differential equation (1) where $[H]_0$, $[G]_0$ and $[HG]_0$ represent the concentration of H and G and HG at time $t$ = 0, led to eqns. (2) and (3), which express the increase or decrease of [HG] as a function of $t$, respectively.[50] Eqn. (2), which represents the association process, is valid at low initial complex concentration, when $[HG]_0$ is smaller than its equilibrium concentration $[HG]_{eq}$. This condition is fulfilled when $[HG]_0 < K_a[H]_0[G]_0$; conversely, eqn. (3), which represents the dissociation, holds when $[HG]_0 > K_a[H]_0[G]_0$.

$$[HG]_t = A \times \coth[Bt + \coth^{-1}(([HG]_0 - D)/A)] + D \quad (2)$$

$$[HG]_t = A \times \tanh[Bt + \tanh^{-1}(([HG]_0 - D)/A)] + D \quad (3)$$

Parameters $A$, $B$ and $D$ in (2) and (3) are themselves defined by relationships (4)–(6).

$$A = -\sqrt{-[H]_0[G]_0 - [H]_0[HG]_0 - [HG]_0[G]_0 + [HG]_0^2 + D^2} \quad \text{(in mol L}^{-1}\text{ or M)} \quad (4)$$

$$B = -k_a \times A \ (\text{in s}^{-1}) \quad (5)$$

$$D = (1/2)[[H]_0 + [G]_0 + 2[HG]_0 + (1/K_a)] \ (\text{in mol L}^{-1}\text{ or M}) \quad (6)$$

In practice, when $K_a$ can be determined by direct measurement of the appropriate equilibrium concentrations, then parameters $A$ and $D$ can be calculated, knowing $[H]_0$, $[G]_0$ and $[HG]_0$. The variation of $[HG]_t$ as a function of $t$ is then fitted to eqns. (2) or (3) to give the unknown parameter $B$, which in turn gives the rate constants $k_a$ and $k_d$ (since $K_a$ is known).[51] Details for the resolution of the kinetic equation are reported in the supplementary information. ‡

### Atomic charge distribution in cryptophanes 1 and 2

Only half of the cryptophane was used in *ab initio* calculations (Gaussian 94, HF, 6.31G*, CHELPG). The inner $CH_2$ of the $O(CH_2)_3O$ bridges being replaced by a terminal $CH_3$ groups to reduce the computation time while keeping the conformational features of the molecules unaffected. In model **2**, the OMe group was replaced by a SMe one, using standard bond lengths and angles for Ar–S–Me and a conformation similar to that of a Ar–O–Me group (*i.e.*, coplanar to the aromatic ring). Since in the crystal structure the geometry of the molecule slightly deviates from ideal $C_3$ symmetry, the calculated charges were averaged over the equivalent atoms or groups, to give the figures shown in Chart 3.

### Syntheses

The starting materials 3-hydroxy-4-methylthiobenzaldehyde **3** (mp 115 °C) and 4-hydroxy-3-methylthiobenzaldehyde **4** (mp 100 °C) were prepared in five steps from vanillin and isovanillin respectively as described previously.[42]

### 1,3-Bis(5-formyl-2-methylthiophenoxy)propane 5

Dibromopropane (2.4 mL; 23.6 mmol) was slowly added to phenol **3** (8 g; 47 mmol) in acetonitrile (80 mL) in the presence of $K_2CO_3$ (6.6 g; 47 mmol). The mixture was refluxed for 12 h. The solvent was stripped off and the residue was taken into water. The resulting solid was washed with aqueous KOH (10% in weight), with water then with diethyl ether. Filtration of the crude material over silica gel (dichloromethane) yielded 7.8 g (88%) of **5**, mp 148 °C (Found: C, 60.42; H, 5.23; S, 17.02. $C_8H_8O_2S$ requires C, 60.61; H, 5.35; S, 17.03%); $\delta_H$ ($CDCl_3$, residual $CHCl_3$ set to 7.24) 9.86 (s, CHO), 7.42 (dd, $J$ 1.5 and 7.9, Ar), 7.32 (d, $J$ 1.5, Ar), 7.16 (d, $J$ 7.9, Ar), 4.35 (t, $J$ 5.9, $OCH_2$), 2.44 (s, $SCH_3$), 2.37 (quintet, $J$ 5.9, $CH_2$). $\delta_C$ ($CDCl_3$, residual $CHCl_3$ set to 77) 191.3 (CHO), 154.9 (ArC–O), 137.9 (ArC–C), 133.6 (ArC–S), 125.2, 123.5, 108.3 (ArC–H), 65.0 ($CH_2O$), 29.0 ($CH_2$), 13.8 ($SCH_3$).

### 1,3-Bis(4-formyl-2-methylthiophenoxy)propane 6

This compound was similarly prepared from phenol **4** (2.58 g; 15.3 mmol) and dibromopropane (0.77 mL; 7.6 mmol) in 30 mL of acetonitrile in the presence of $K_2CO_3$ (2.12 g; 15.3 mmol). Purification was done by digestion of the solid in hot dichloro-

methane, giving 2.25 g (78%) of pure **6**, mp 195 °C (Found: C, 59.26; H, 5.29; S, 16.47. $C_8H_8O_2S$ + 0.5 $H_2O$ requires C. 59.19; H, 5.49; S, 16.63%); $\delta_H$ ($CDCl_3$, residual $CHCl_3$ set to 7.24) 9.84 (s, CHO), 7.62 (d, *J* 1.9, Ar), 7.58 (dd, *J* 1.9 and *J* 8.3, Ar), 6.96 (d, *J* 8.3, Ar), 4.37 (t, *J* 5.9, $OCH_2$), 2.45 (s, $SCH_3$), 2.41 (quintet, *J* 5.9, $CH_2$); $\delta_C$ ($CDCl_3$, residual $CHCl_3$ set to 77) 190.6 (CHO), 159.7 (ArC–O), 130.4 (ArC–C), 129.9 (ArC–S), 129.7, 124.6, 110.3 (ArC–H), 65.1 ($CH_2O$), 28.9 ($CH_2$), 14.1 ($SCH_3$).

#### 1,3-Bis(5-hydroxymethyl-2-methylthiophenoxy)propane 7

Reduction of dialdehyde **5** (7.8 g; 20.7 mmol) was carried out in 200 mL of methanol by reaction with 3.9 g of $NaBH_4$ at room temperature overnight. The methanol was stripped off, the solid was taken into water and collected by suction filtration. Yield 6.9 g (87%) of pure **7**, mp 133 °C (Found: C, 60.05; H, 6.33; S, 16.50. $C_{19}H_{24}O_4S_2$ requires C. 59.97; H, 6.35; S, 16.85%); $\delta_H$ ($CDCl_3$, residual $CHCl_3$ set to 7.24) 7.08 (d, *J* 8.1, Ar), 6.96 (s, Ar), 6.90 (d, *J* 8.1, Ar), 4.58 (d, *J* 6, $CH_2OH$), 4.58 (t, *J* 6, $OCH_2$), 2.39 (s, $SCH_3$), 2.33 (quintet, *J* 6, $CH_2$), 1.67 (t, *J* 6, OH); $\delta_C$ (DMSO $d_6$, residual DMSO set to 39.6) 153.6 (ArC–O), 135.5 (ArC–C), 126.7 (ArC–S), 123.8, 123.6, 111.2 (ArC–H), 64.9 ($CH_2OH$), 62.7 ($CH_2O$), 30.8 ($CH_2$), 13.5 ($SCH_3$).

#### 1,3-Bis(4-hydroxymethyl-2-methylthiophenoxy)propane 8

The reduction of **6** (2.18 g; 5.8 mmol) was carried out in 50 mL of methanol by reaction with 3.3 g (87 mmol) of $NaBH_4$ at reflux for 48 h. The methanol was stripped off, the solid was taken into water and collected by suction filtration. Yield 1.7 g (77%) of pure **8**, mp 157 °C (Found: C, 59.53; H, 6.32; S, 16.75. $C_{19}H_{24}O_4S_2$ requires C, 59.97; H, 6.35; S, 16.85%); $\delta_H$ (DMSO $d_6$, residual DMSO set to 2.49) 7.07 (s, Ar), 7.03 (d, *J* 8.1, Ar), 6.91 (d, *J* 8.1, Ar), 5.07 (t, *J* 5.6, OH), 4,41 (d, *J* 5.6, $CH_2OH$), 4.19 (t, *J* 6, $OCH_2$), 2.34 (s, $SCH_3$), 2.14 (quintet, *J* 6, $CH_2$); $\delta_C$ (DMSO $d_6$, residual DMSO set to 39.6) 155.5 (ArC–O), 138.8 (ArC–C), 126.6 (ArC–S), 125.7, 119.7, 110.1 (ArC–H), 65 ($CH_2OH$), 65 ($CH_2O$), 29.3 ($CH_2$), 14.5 ($SCH_3$).

#### Cryptophane 2 from 7

A mixture of diol **7** (2 g; 5.25 mmol) in $CHCl_3$ (4 mL) and formic acid (240 mL) was placed in a 500 mL rotatory evaporator flask and heated in the water bath at 60 °C for 6 h, with slow rotation (a precipitate began to form after 3 h). Evaporation to dryness under vacuum gave a residue from which the desired cryptophane **2** was isolated by column chromatography ($CH_2Cl_2$). Yield 39 mg (2.1%) of **2** (solid, no mp) (Found: C, 57.45; H, 5.18. $C_{57}H_{60}O_6S_6$ + 2.5 $CH_2Cl_2$ requires C, 57.36; H, 5.26%); $\delta_H$ ($CDCl_3$, residual $CHCl_3$ set to 7.24) 6.84 (s, ArH *ortho* to $SCH_3$), 6.49 (s, ArH *ortho* to $OCH_3$), 4.64 (d, *J* 14, $CH_a$), 4.08 and 3.85 (two m, $OCH_2$), 3.47 (d, *J* 14, $CH_e$), 2.37 (s, $SCH_3$), 2.22 (m, $CH_2$); $\delta_C$ ($CDCl_3$, residual $CHCl_3$ set to 77) 153.8 (ArC–O), 135.8, 131.8 (ArC–C), 125.4 (ArC–S), 125.2, 110.8 (ArC–H), 63.8 ($CH_2O$), 36.4 (Ar–$CH_2$–Ar), 30.2 ($CH_2$), 17.8 ($SCH_3$); *m/z* (FAB) 1033.3 ($M^+$. $C_{57}H_{60}O_6S_6$ requires 1033.49).

#### Cryptophane 2 from 8

Similarly, a mixture of diol **8** (1.6 g; 4.2 mmol) in $CHCl_3$ (8 mL) and formic acid (200 mL) was stirred at 60 °C for 6 h. The same chromatographic purification procedure as above gave 20 mg (1.4%) of cryptophane **2** showing the same physical and spectroscopic properties as the sample obtained from **7**.

## Acknowledgements

We are grateful to Professor J. Vidal and Dr D. Sakellariou for their assistance in the development of the kinetic model used in this work.

## References

1 D. J. Cram and J. M. Cram, *Container Molecules and Their Guests*, The Royal Society of Chemistry, Cambridge, ed. J. F. Stoddart, 1994.
2 E. Maverick and D. J. Cram, in *Comprehensive Supramolecular Chemistry*, ed. F. Vögtle, Pergamon, 1996, vol. 2, pp. 367–418.
3 J. Rebek Jr., *Chem. Soc. Rev.*, 1996, 255–264.
4 D. M. Rudkevich, G. Hilmersson and J. Rebek Jr., *J. Am. Chem. Soc.*, 1998, **120**, 12216–12225.
5 D. M. Rudkevich and J. Rebek Jr., *Eur. J. Org. Chem.*, 1999, 1991–2005.
6 A. Jasat and J. C. Sherman, *Chem. Rev.*, 1999, **99**, 931–967.
7 N. Chopra and J. C. Sherman, *Angew. Chem., Int. Ed. Engl.*, 1999, **38**, 1955–1957.
8 N. Chopra, C. Naumann and J. C. Sherman, *Angew. Chem., Int. Ed. Engl.*, 2000, **39**, 194–196.
9 S. D. Starnes, D. M. Rudkevich and J. Rebek Jr., *J. Am. Chem. Soc.*, 2001, **123**, 4659–4669.
10 A. M. A. van Wageningen, P. Timmerman, J. P. M. van Duynhoven, W. Verboom, F. C. J. M. van Weggel and D. N. Reinhoudt, *Chem. Eur. J.*, 1997, **3**, 639–654.
11 C. L. D. Gibbs, E. D. Stevens and B. C. Gibb, *Chem. Commun.*, 2000, 363–364.
12 C. L. D. Gibbs, H. Xi, P. A. Politzer, M. Concha and B. C. Gibb, *Tetrahedron*, 2002, 673–681.
13 L. J. Prins, D. N. Reinhoudt and P. Timmerman, *Angew. Chem., Int. Ed.*, 2001, **40**, 2382–2426.
14 M. O. Vysotsky, I. Thondorf and V. Böhmer, *Chem. Commun.*, 2001, 1890–1891.
15 L. J. Prins, F. De Jong, P. Timmerman and D. N. Reinhoudt, *Nature*, 2000, **408**, 181–184.
16 M. Fujita, K. Umemoto, M. Yoshizawa, N. Fujita, T. Kusukawa and K. Biradha, *Chem. Commun.*, 2001, 509–518.
17 A. Collet, in *Comprehensive Supramolecular Chemistry*, ed. F. Toda, Pergamon, 1996, ch. 9, Vol. 6, pp. 281–303.
18 A. Collet, in *Comprehensive Supramolecular Chemistry*, ed. F. Vögtle, Pergamon, 1996, ch. 11, vol. 2, pp. 325–365.
19 F. Diederich, *Cyclophanes*, ed. J. F. Stoddart, Royal Society of Chemistry, Cambridge, 1991.
20 L. Garel, J.-P. Dutasta and A. Collet, *Angew. Chem., Int. Ed.*, 1993, **32**, 1169–1171.
21 J. Canceill, L. Lacombe and A. Collet, *J. Am. Chem. Soc.*, 1985, **107**, 6993–6996.
22 J. Canceill, L. Lacombe and A. Collet, *J. Am. Chem. Soc.*, 1986, **108**, 4230–4232.
23 J. Canceill, M. Cesario, A. Collet, J. Guilhem, L. Lacombe, B. Lozach and C. Pascard, *Angew. Chem., Int. Ed.*, 1989, **28**, 1246–1248.
24 L. Garel, H. Vezin, J.-P. Dutasta and A. Collet, *J. Chem. Soc., Chem. Commun.*, 1996, 719–720.
25 L. Garel, J.-P. Dutasta and A. Collet, *New J. Chem.*, 1996, **20**, 1265–1271.
26 A. Collet, J.-P. Dutasta and B. Lozach, *Bull. Soc. Chim. Belg.*, 1990, **99**, 617–633.
27 L. Garel, B. Lozach, J.-P. Dutasta and A. Collet, *J. Am. Chem. Soc.*, 1993, **115**, 11652–11653.
28 J. Lang, J. J. Dechter, M. Effemey and J. Kowalewski, *J. Am. Chem. Soc.*, 2001, **123**, 7852–7858.
29 K. Bartik, M. Luhmer, J.-P. Dutasta, A. Collet and J. Reisse, *J. Am. Chem. Soc.*, 1998, **120**, 784–791.
30 M. Luhmer, B. M. Goodson, Y.-Q. Song, D. D. Laws, L. Kaiser, M. C. Cyrier and A. Pines, *J. Am. Chem. Soc.*, 1999, **121**, 3502–3512.
31 T. Brotin, A. Lesage, L. Emsley and A. Collet, *J. Am. Chem. Soc.*, 2000, **122**, 1171–1174.
32 T. Brotin, T. Devic, A. Lesage, L. Emsley and A. Collet, *Chem. Eur. J.*, 2001, **7**, 1561–1573.
33 P. D. Kirchhoff, M. B. Bass, B. A. Hanks, J. M. Brigss, A. Collet and J. A. McCammon, *J. Am. Chem. Soc.*, 1996, **118**, 3237–3246.
34 P. D. Kirchhoff, J.-P. Dutasta, A. Collet and J. A. McCammon, *J. Am. Chem. Soc.*, 1997, **119**, 8015–8022.
35 A. Varnek, G. Wipff and A. Collet, *J. Comput. Chem.*, 1998, **19**, 820–832.
36 P. D. Kirchhoff, J.-P. Dutasta, A. Collet and J. A. McCammon, *J. Am. Chem. Soc.*, 1999, **121**, 381–390.
37 B. Lozach, Thèse de Doctorat, Université Lyon 1, 1990. See also references 26,27.
38 D. A. Dougherty, *Science*, 1996, **271**, 163–168; J. C. Ma and D. A. Dougherty, *Chem. Rev.*, 1997, **97**, 1303–1324.
39 H.-J. Schneider, T. Blatter, S. Simova and I. Theis, *J. Chem. Soc., Chem. Commun.*, 1989, 580–581.

40 S. Roelens and R. Torriti, *J. Am. Chem. Soc.*, 1998, **120**, 12443–12452.
41 J. Canceill and A. Collet, *J. Chem. Soc., Chem. Commun.*, 1988, 163–166.
42 C. Garcia, C. Andraud and A. Collet, *Supramol. Chem.*, 1992, **1**, 31–45.
43 A. Tambuté, J. Canceill and A. Collet, *Bull. Chem. Soc. Jpn.*, 1989, **62**, 1390–1392.
44 This feature was observed in the X-ray crystal structure of $CHCl_3$@**1** (reference 23).
45 The apparent slowness is in fact due to the large frequency difference of the exchanging species resonances, $\Delta\delta = 4.4$ ppm *i.e.* $\Delta\nu = 2200$ Hz at 500 MHz, which makes exchange processes having rate constants smaller than $\pi\Delta\nu/\sqrt{2} = 4.9\ 10^3\ s^{-1}$ slow on the spectrometer time scale.
46 M. L. Martin, G. Martin, J.-J. Delpuech, in *Practical NMR Spectroscopy*, Heyden & Son Ltd., London, 1980.
47 SYBYL 6.3 from Tripos, 1699 S. Hanley Road, St Louis, MO 63144–2913.
48 The NMR chemical shift of the picrate anion in the complex indicates that the anion is free in solution and does not interact strongly with the host molecule (a high field shift of 0.07 ppm was observed independently of the concentrations of salt and host). Thus, an important counterion effect was excluded and only the entropic contribution essentially due to solvation and ion pair dissociation prevail.
49 S. Bartoli and S. Roelens, *J. Am. Chem. Soc.*, 2002, **124**, 8307–8315.
50 This differential equation is generally integrated under conditions where it can be simplified, *e.g.*, $[H]_0 = [G]_0$ and $[HG]_0 = 0$. We were unable to find any earlier example of its integration in a general case such as this discussed here.
51 When $K_a$, is unknown or not measurable, a multivariable fitting of the variation of $[HG]_t$ to eqns. (2) or (3) may in principle provide all the unknown parameters, $A$, $B$ and $D$, from which the rate constants and equilibrium constant can be derived. This procedure, which requires data of exceptional quality, was not employed in the present work.